

ESTIMATION OF CHLORIDE DIFFUSION COEFFICIENT AND TORTUOSITY FACTOR FOR MUDSTONE

By F. S. Barone,¹ R. K. Rowe² and R. M. Quigley,³ Members, ASCE

ABSTRACT: An experimental estimation of the chloride diffusion coefficient and the corresponding tortuosity factor for a saturated, intact mudstone is described. Laboratory tests simulating one-dimensional diffusive transport are performed by placing distilled water directly above Bison mudstone specimens having high chloride porewater concentrations. Chloride and other species naturally occurring in the pore water are then permitted to diffuse out of the sample and into the distilled water reservoir for a period of up to 34 days. At the end of the test, the sample is sectioned, and the chloride pore water concentration profile is measured. Fickian diffusion theory is then used to deduce the chloride diffusion coefficient. The diffusion coefficient at a temperature of 10° C ranges from 1.5 to 2.0 × 10⁻⁶ cm²/s, from which a tortuosity factor ranging from 0.15 to 0.20 can be calculated. For comparison, an attempt is made to obtain the diffusion coefficient for bromide diffusing into the sample simultaneous with chloride diffusing out. It is found, however, that the concentration profile obtained for bromide cannot be fitted by the diffusion theory, due to interactions between bromide and other species naturally occurring in the rock sample.

INTRODUCTION

The evaluation of contaminant transport from waste disposal sites or subsurface chemical repositories located in fractured rock requires consideration of advective-dispersive transport along the fractures and diffusive transport from the fractures into the surrounding rock matrix. Advective-dispersive transport along the fractures represents the dominant mode of contaminant migration from such facilities. The process of matrix diffusion allows contaminants to be stored in micropores, where they are essentially immobile relative to their potential migration along fractures. For reactive contaminants, matrix diffusion also serves to increase the amount of solid available for interaction, beyond that provided by the surface area of the fracture walls. The net effect of matrix diffusion is to retard the arrival of both reactive and nonreactive contaminants at any point along the fracture [see Freeze and Cherry (1979) for a general discussion].

In order to mathematically model contaminant transport along fractures with diffusion into the rock matrix, it is necessary to estimate the diffusion coefficient of the contaminant in the rock matrix [e.g., see Rowe and Booker (1989)]. For practical purposes, the diffusion coefficient of a species in a saturated porous media (D) may be estimated by the empirical expression

$$D = \tau \times D_o \dots\dots\dots (1)$$

¹Proj. Engr., Golder Associates, 2180 Meadowvale Blvd., Mississauga, Ontario, Canada, L5N-5S3; formerly, Grad. Student, Univ. of Western Ontario, London, Ontario, Canada.

²Prof., Geotech. Res. Ctr., Faculty of Engrg. Sci., The Univ. of Western Ontario, London, Ontario, Canada N6A 5B9.

³Prof., Geotech. Res. Ctr., Faculty of Engrg. Sci., The Univ. of Western Ontario, London, Ontario, Canada N6A 5B9.

Note. Discussion open until December 1, 1992. To extend the closing date one month, a written request must be filed with the ASCE Manager of Journals. The manuscript for this paper was submitted for review and possible publication on March 10, 1990. This paper is part of the *Journal of Geotechnical Engineering*, Vol. 118, No. 7, July, 1992. ©ASCE, ISSN 0733-9410/92/0007-1031/\$1.00 + \$.15 per page. Paper No. 26647.

where D_o = the diffusion coefficient of the species in pure aqueous solution; and τ = the tortuosity of the porous media. The aqueous-solution diffusion coefficient may be obtained from the literature [e.g., *American* (1972); Wilke and Chang (1955)]. The tortuosity factor can be considered as a correction factor ($0.0 < \tau < 1.0$), which accounts for the fact that pathways for diffusion in a porous media are longer and more tortuous than in aqueous solution. Although only approximately true [see Quigley et al. (1987)], the tortuosity is often assumed to be a property of the porous media, depending on fabric and pore structure rather than the nature of the diffusing species. Hence, by means of (1), it is often calculated using diffusion coefficient data obtained from laboratory diffusion experiments for simple nonreactive species such as chloride (Cl^-). The purpose of this paper is to present a laboratory estimation Cl^- diffusion coefficient and corresponding tortuosity factor on samples of Bison mudstone, by means of a simple nonsteady-state diffusion test technique. In practice, the tortuosity factor obtained by this technique may be useful in estimating the diffusion coefficient of other species provided that the diffusion coefficient in aqueous solution (D_o) is known.

In a previous study (Barone et al. 1990), a similar method was used to estimate the chloride diffusion coefficient and tortuosity factor on samples of intact, saturated, Queenston shale. Unlike the Queenston shale, the Bison mudstone shows a significant amount of moisture uptake at the end of the diffusion test. Hence, a second objective is to discuss this increase in moisture content and its effect on the measured chloride diffusion coefficient. Finally, results of a slightly modified technique, designed to yield the matrix diffusion coefficient for chloride and bromide (Br^-) simultaneously on a single sample, are presented.

THEORETICAL DEVELOPMENT

One-dimensional diffusive transport of a dissolved nonreactive species through a saturated porous medium may be approximated by Fick's second law viz.

$$\frac{\partial c}{\partial t} = D \frac{\partial^2 c}{\partial z^2} \dots\dots\dots (2)$$

where c = the species concentration in the pore water at time t and depth z ; and D = the porous media diffusion coefficient for the solute. It should be noted that the concentration term, c , refers to the mass of solute per unit volume of pore water that is accessible to the diffusing species. This is important for very dense porous media where a portion of the pore water may not be accessible to the diffusing solute due to exclusion from the vicinity of the negatively charged clay surfaces, and/or due to pores being too small to accommodate the hydrated solute.

In the tests conducted by the writers, a known volume of distilled water was placed in contact with a core sample of intact, saturated Bison mudstone, as shown in Fig. 1. Chloride and other species naturally occurring in the pore water of the mudstone were then permitted to diffuse upwards into the distilled water reservoir. Under these conditions, it can be shown (Rowe and Booker 1985) that the concentration of chloride $c_T(t)$ in the reservoir at any time t is given by

$$c_T(t) = \frac{1}{H_f} \int f_T(t) dt \dots\dots\dots (3)$$

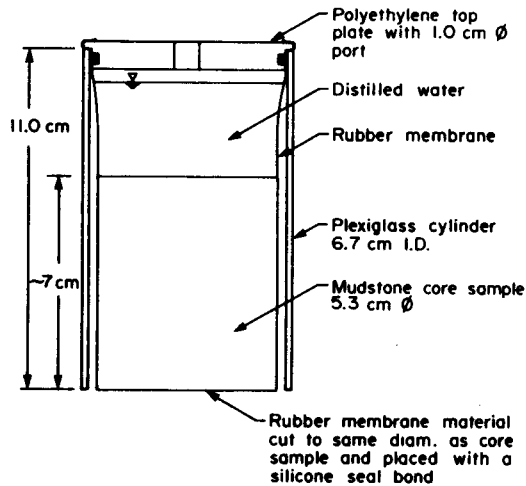


FIG. 1. Schematic Diagram of Assembled Diffusion Model

where H_f = the height of distilled water calculated as the volume of distilled water divided by the cross-sectional area of the core sample perpendicular to the direction of diffusion; and $f_T(t)$ = the mass flux across the boundary between the reservoir and the sample. The subscript T refers to the top of the sample. The mass flux $f_T(t)$ can be further related to the chloride concentration gradient across the sample/reservoir boundary $[\partial c(t)/\partial z]_T$ by Fick's first law, viz.

$$f_T(t) = n' D \left(\frac{\partial c(t)}{\partial z} \right)_T \dots \dots \dots (4)$$

where n' = the porosity available for chloride diffusion within the sample. As previously noted, for very compact porous media, a portion of the porewater may not be accessible to the diffusing solute due to exclusion from the vicinity of the negatively charged clay surfaces and/or due to pores not being large enough to accommodate the solute. Hence, the term n' , often referred to as the effective or transport porosity, may be lower than the total porosity n calculated from the moisture content.

The base of the sample is sealed with an impermeable membrane so as to create a zero flux base boundary condition; that is

$$f_B(t) = n' D \left(\frac{\partial c(t)}{\partial z} \right)_B = 0 \dots \dots \dots (5)$$

One-dimensional diffusion of chloride through the mudstone sample is thus described by (2)–(5). The solution to these equations has been given by Rowe and Booker (1985) and has been implemented in the computer program POLLUTE (Rowe and Booker 1990). This approach permits accurate calculation of concentration in only a few seconds on a microcomputer and, hence, is well suited for use in interpretation of the experimental results.

After allowing time for outwards diffusion (~31 days), the sample was

sectioned and the chloride concentration profile with depth was determined. Program POLLUTE was then used to obtain a match to the experimental Cl^- profile by varying the diffusion coefficient (while keeping other geometrical and material parameters constant). It should be noted that the initial Cl^- porewater concentration profile used in the analysis was linearly interpolated from the measured Cl^- concentration on background samples taken from directly above and below the test sample. The diffusion coefficient that was judged to provide the best fit to the experimental profile was selected as the experimental chloride diffusion coefficient.

A second type of test, designed to simultaneously yield a diffusion coefficient for both chloride and bromide, involved spiking the distilled water reservoir with potassium bromide. For this case, diffusion of bromide into the sample is described by (2)–(5), with the exception that the upper boundary condition [(3)] is taken as

$$c_T(t) = c_o - \frac{1}{H_T} \int f_T(t) dt \dots\dots\dots (6)$$

where c_o = the Br^- concentration in the reservoir at the start of the test.

BISON MUDSTONE

Core samples of Bison mudstone (5.3-cm diameter) were obtained from a site near Oklahoma City, Oklahoma. Upon removal from the ground, the core samples were wrapped with aluminum foil and coated with paraffin wax in order to maintain their natural moisture content. On arrival at the University of Western Ontario Laboratory, the core samples were stored at 10° C prior to use. Typically, the diffusion tests were started 28–45 days after coring. All specimens chosen for diffusion testing were free of visual fractures.

A total of five specimens (≈ 7 cm in length) were selected for the diffusion tests (Sa 1–5). The depth below ground surface, geotechnical index characteristics, and mineralogy are summarized for each test sample in Tables 1 and 2. The data given for moisture content represent average values obtained from two (1-cm thick) core sections, one cut directly above and one cut directly below the test specimen. Specific gravity, dry density, and mineralogy were determined on a single sample from either directly above or below the test sample.

The degree of saturation for each sample was calculated based on dry density, moisture content, and specific gravity. The dry density was measured on approximately 5 g of intact, freeze-dried mudstone, using a Mi-

TABLE 1. Physical Characteristics of Bison Mudstone Samples (Average Values)

Sample (1)	Depth below ground surface (m) (2)	Moisture content (%) (3)	Specific gravity (4)	Dry density (g/cm ³) (5)	Degree of saturation (%) (6)	Total porosity (%) (7)
1	44.1	10.46	2.73	2.11	98	22.56
2	44.8	10.70	2.81	2.17	100	23.12
3	43.0	12.18	2.81	2.09	99	25.69
4	85.2	9.00	2.77	2.17	91	21.50
5	95.8	11.14	2.76	2.09	99	23.70

TABLE 2. Mineralogical Composition of Bison Mudstone

Sample (1)	% Quartz (2)	% Calcite (3)	% Dolomite (4)	% Na- Feldspar (5)	% Illite (6)	% Chlo- rite and smectite ^a (7)	Cation exchange capacity (meq/100 g solids) (8)
1	28	1	8	8	34	21	27
2	12	2	12	4	37	33	35
3	17	2	7	3	40	31	41
4	36	<1	6	4	30	24	44
5	34	<1	5	7	25	29	43

^aInterlayered with illite.

chromeritics Mercury Porosimeter. The degree of saturation calculated this way ranged from 98% to 100% for all samples except sample 4, which gave a value of 91%. The moisture content, specific gravity, and the degree of saturation were then used to calculate the total porosity, *n*.

For each test sample, the background concentrations for various dissolved and adsorbed inorganic species are summarized in Table 3. Again, the values given represent average values based on the two core slices cut above and below the test sample. Dissolved concentrations were obtained by a single washing of 8 g of oven-dried, pulverized (<76 μm) mudstone in 50 mL of distilled water. The mixture was agitated for about 15 min and centrifuged at 2,500 rpm for 30 min. The supernatant was then analyzed for the species of interest. Chloride concentration in the supernatant was measured by a specific ion electrode, sulphate by ion chromatography, and the cations by atomic absorption spectrometry. It was found that the supernatant concentrations obtained for chloride upon washing the pulverized mudstone for approximately 15 min was not significantly different than that obtained upon washing for 24 hr, indicating that the wash duration of 15 min was adequate.

Supernatant concentration was converted to pore water concentration using the relationship

$$\text{pore water concentration (g/L)} = \frac{cV\rho}{mw} \dots\dots\dots (7)$$

where *c* = species concentration in the supernatant (g/L); *V* = volume of supernatant (L); *m* = mass of oven-dried sample used in the wash (g); *w* = moisture content of slice prior to oven-drying; and *ρ* = density of pure water at 22° C (1,000 g/L).

It should be noted again that pore water concentrations calculated using (7) represent the dissolved mass of the species per unit volume of total pore water, which includes adsorbed water and water within pores too small to accommodate the diffusing species.

Adsorbed cation concentrations (see Table 2) were measured by washing 1.5 g of air-dried, powdered material in 50 mL Silver Thiourea solution (pH = 7.0) for about 24 hr. With this technique, any adsorbed cations on the clay exchange sites are replaced by the silver ion from the wash solution (Chabbra 1975). The mixture was then centrifuged and the supernatant analyzed for the cations by atomic absorption spectrometry. The sum of the

TABLE 3. Chemical Characteristics of Mudstone (Average Values)

Sample (1)	Porewater Species (g/L)						Sum of porewater species molar concentrations (moles/L) (8)	Adsorbed Species (meq/100 g)			
	Cl ⁻ (2)	SO ₄ ⁻ (3)	Na ⁺ (4)	K ⁺ (5)	Ca ⁺⁺ (6)	Ng ⁺⁺ (7)		Na ⁺ (9)	K ⁺ (10)	Ca ⁺⁺ (11)	Mg ⁺⁺ (12)
1	2.69	4.62	4.64	0.93	<0.06	0.17	0.36	4.42	2.92	11.33	8.07
2	1.50	4.52	4.00	1.75	<0.06	0.26	0.32	6.95	3.73	14.55	9.90
3	1.64	4.53	4.09	1.29	<0.05	0.20	0.31	7.68	7.80	14.60	10.73
4	5.17	5.20	5.83	1.85	<0.04	0.32	0.51	6.94	3.05	18.10	15.50
5	5.35	5.52	6.28	2.10	<0.03	0.38	0.55	7.00	3.60	16.95	15.20

Adsorbed cation concentrations given in Table 3 is considered to be representative of the cation exchange capacity (see Table 2).

EXPERIMENTAL PROCEDURES

As shown in Fig. 1, the diffusion model consists of a hollow Plexiglas cylinder with an inside diameter of 6.7 cm and length of approximately 11 cm. The diffusion test specimens (≈ 7 cm in length) were cut from core sections using an oil-lubricated diamond saw and immediately wiped free of oil using ethanol. Each test specimen was then coated along its sides with silicone seal and fitted with a tight rubber membrane extending from the bottom to about 5 cm above the top of the specimen. The rubber membrane serves to prevent drying along the sides and allows for the containment of a reservoir on the top of the specimen. Placement of the silicone seal along the sides of the sample helps to ensure a good seal along the membrane-sample interface. To prevent drying through the bottom, a circular piece of rubber membrane material was cut to the same diameter as the specimen and adhered to the bottom using a silicone seal bond. The specimen was then placed within the Plexiglas cylinder and the upper part of the membrane folded over the top of the cylinder, forming a reservoir compartment directly above the sample. The top of the cylinder was then fitted with a polyethylene cap plate and the entire model transferred to a controlled environmental chamber where it was maintained at a constant temperature of 10° C for a period of about 31 days. During this period, the reservoir solution was mixed periodically so as to maintain a relatively uniform concentration throughout the reservoir depth.

At the end of each test, the rock sample was removed and sectioned into six segments using an oil-lubricated diamond saw. Immediately, each slice was wiped free of oil using ethanol, weighed, and placed into a 100° C oven for at least 48 hr for determination of average moisture content (w). The vertical distribution of chloride concentration was measured by pulverizing each oven-dried slice to $<76 \mu\text{m}$ and then washing the chloride out using the distilled water wash technique previously described.

Calculation of the Cl^- pore water concentration from that measured in the supernatant was performed using (7), taking the w term as the moisture content measured for the slice at the end of the diffusion test. The resultant Cl^- concentration profile with depth, was then fitted using program POLLUTE, taking the effective porosity, n' , as equal to the total porosity distribution obtained at the end of the test. The diffusion coefficient judged to provide the best fit to the experimental profile was selected as the experimental chloride diffusion coefficient.

For the test in which the distilled water reservoir was spiked with reagent-grade potassium bromide, the bromide concentration profile at the end of the test was obtained using (7) and the same wash technique used for chloride. The only difference was that the bromide concentration in the wash supernatant was measured by ion chromatography. The theoretical analysis of the bromide profile was also conducted using the program POLLUTE, taking the effective porosity equal to the total porosity distribution at the end of the test.

TESTS CONDUCTED

A diffusion test was conducted on each of the five specimens described in Table 1. For sample 5, the reservoir solution contained 2.2 g/L potassium

bromide to permit determination of the diffusion coefficient for bromide diffusing into the sample simultaneously with chloride diffusing out. Table 4 shows those details of each test that are pertinent to the theoretical analysis.

EXPERIMENTAL RESULTS AND INTERPRETATION

Moisture Content after Diffusion

For each specimen, the moisture content profile at the end of the diffusion period is shown on Fig. 2. Also shown are the initial profiles inferred from moisture contents measured on the background slices above and below the test sample.

Comparison of the initial and final profiles suggests that some moisture uptake had occurred in each test. The increase in moisture content may be attributed to: initial negative pore pressures resulting from the relief of in situ total stresses, osmotic water migration from the reservoir into the sam-

TABLE 4. Specific Details Pertinent to Theoretical Analysis of Each Test

Sample number (1)	Sample height (cm) (2)	H_f (cm) (3)	Test duration (days) (4)	Background Cl^- concentration ^a (g/L) (5)	Total porosity ^a (6)
1	7.1	3.0	31	2.90; 2.48	22.5; 22.7
2	7.0	3.1	34	1.48; 1.51	23.3; 23.0
3	7.0	3.1	32	1.76; 1.52	26.1; 25.2
4	7.0	3.1	31	5.04; 5.30	21.4; 22.0
5	5.7	3.6	31	5.06; 5.63	24.6; 22.7

^aMeasured on a core section taken directly (above; below) the test sample.

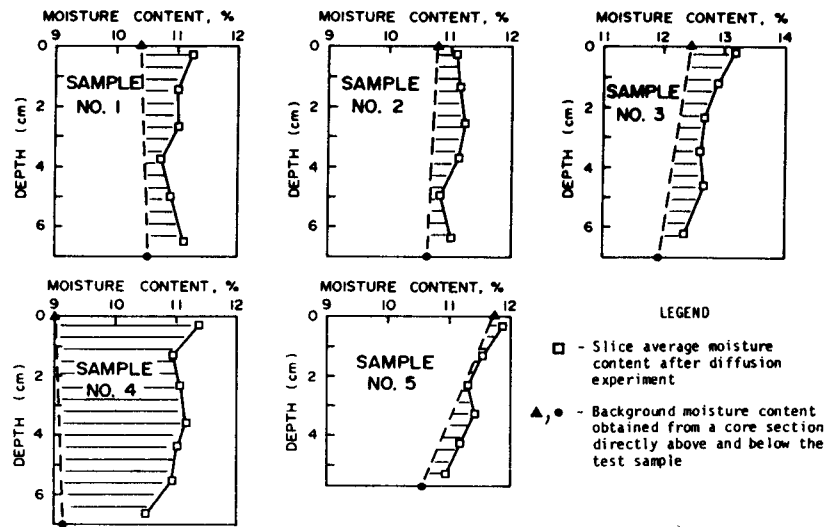


FIG. 2. Moisture Content Increases with Depth after Diffusion

ple, and the swelling of clay double layers. First, the relief of total stress upon sampling may have produced an initial negative pore pressure throughout the specimen. When the specimen is exposed to water, as in the tests conducted, the negative pore pressure would be relieved by moisture uptake, resulting in an increase in moisture content throughout the entire sample. Second, osmotic water migration from the reservoir into the sample may have occurred in response to the initially low total ion concentration of the reservoir solution relative to the bulk pore fluid. Finally, the decrease in total ion concentration of the bulk pore fluid (due to diffusion into the reservoir) may have led to swelling of the clay double layers. The net effect of this mechanism would be an increase in repulsive pressure between the clay particles [e.g., see Mitchell (1976)] and subsequent swelling of the sample. It should be noted, however, that the absence of a more dominant moisture content increase near the sample-reservoir interface (where the depletion of pore water ions is largest) suggests that the influence of this mechanism is probably small in comparison to the previous two.

Considering each test sample to be completely saturated at the end of the diffusion test, the percentage volume change corresponding to the moisture content increase was calculated. Samples 1–3 yielded a percentage volume change ranging from 0.50% to 0.56%. Since samples 1–3 were taken from similar depths (Table 1) and have similar pore water chemistries (Table 3), the swelling mechanisms should lead to similar volume changes, which is the case. For sample 4, the percentage volume change (1.6%) was significantly higher. This may be explained by the greater sample depth and higher pore water species concentrations for sample 4, which would augment stress relief swelling and osmotic water migration into the sample, respectively. Furthermore, sample 4 was drier than the rest of the samples and probably in a state of greater water deficiency (see Table 1). For sample 5, which was tested using a reservoir solution of 2.2 g/L KBr rather than pure distilled water, the percentage volume change (0.23%) was the least, despite the similarities in depth and pore water chemistry with sample 4. Although part of the increases in moisture content were probably suppressed in the upper part of this sample by the more saline reservoir, potassium diffusing into the sample may also have contributed. Adsorption of lesser hydrated potassium onto the exchange sites at the expense of sodium (as will be illustrated later) would cause the clay double layers to contract, thus, inhibiting swelling.

For the diffusion tests conducted, the significance of sample swelling lies in its effect on the observed concentration profile and, in turn, the measured diffusion coefficient for the species of interest. This will be discussed in the following section.

Determination of Chloride Diffusion Coefficient

The Cl^- concentration profiles at the end of each test, obtained using the wash technique, are presented in Fig. 3. The uppermost data point on the profiles presents the measured Cl^- concentration in the distilled water reservoir at the end of the test. Also presented are the initial Cl^- concentration profiles inferred from the Cl^- concentration of background slices from above and below the specimen. To establish the test method variability in the Cl^- pore water concentration measurements, a wash extraction was performed on three powdered samples from selected slices of samples 2 and 4. The spreads in values are indicated by means of a range bar. This exercise indicated a maximum uncertainty of about $\pm 6\%$. As a check on the ex-

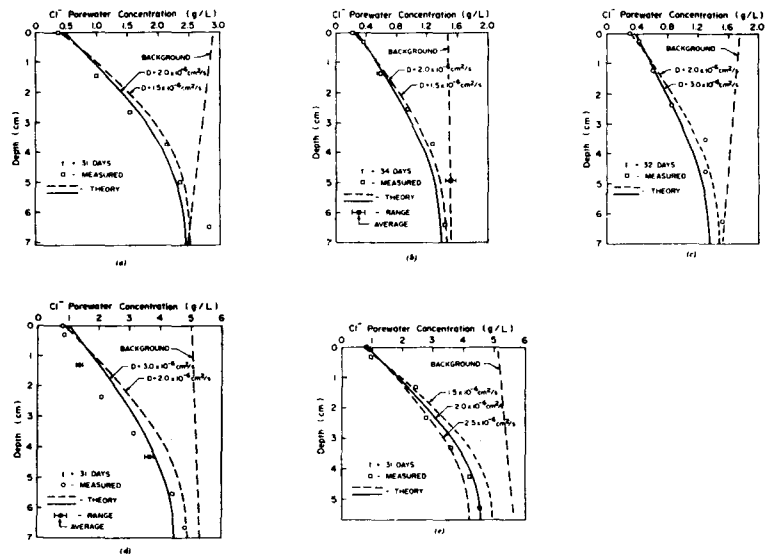


FIG. 3. Chloride Pore Water Concentration Variation with Depth: (a) Sample 1; (b) Sample 2; (c) Sample 3; (d) Sample 4; (e) Sample 5

perimental technique, the percentage recovery of Cl^- (i.e., the ratio of Cl^- mass recovered at the end of the test to the total Cl^- mass at the start of the test) was calculated. The Cl^- mass at the start of the test was inferred from the background Cl^- concentrations above and below the test sample. For all tests, the deviation from 100% recovery was within $\pm 3\%$.

The chloride pore water concentration data shows a significant decrease with respect to the background concentration, as a result of diffusion upwards into the distilled water reservoir. In order to maintain electroneutrality, the upward migration of chloride into the distilled water reservoir is coupled predominantly by the upward migration of sodium. This is indicated in Table 5, which shows the concentration of various species in the distilled water reservoir at the end of each test.

Values of experimental diffusion coefficient and corresponding tortuosity factor obtained for each sample are presented in Table 6. For a temperature of 10°C , the experimental Cl^- diffusion coefficient varied from 1.5 to $2.0 \times 10^{-6} \text{ cm}^2/\text{s}$, which corresponds to a tortuosity ranging from 0.15 to 0.20 . It should be noted that the tortuosity factor [i.e., $(D/D_o)_{\text{Cl}^-}$] was calculated taking D_o as $0.99 \times 10^{-5} \text{ cm}^2/\text{s}$. This value of D_o represents an approximate aqueous diffusion coefficient for both Na^+ and Cl^- at 10°C when diffusing together from a source solution containing about 0.3 Molar NaCl (American 1972).

Except for sample 4, which showed the greatest swelling, the test specimens provided a diffusion profile that could be adequately fitted by the theoretical model, suggesting that the observed swelling had little effect on the concentration profile developed at the end of the test. For these samples, the scatter of the chloride data about the best-fit theoretical curve appears to be random and representative of the uncertainty in the wash extraction procedure used. The experimental data from sample 4, however, show a distinct trend of deviation from the theoretical curves that cannot be ex-

TABLE 5. Reservoir Concentrations at End of Each Test

Sample number (1)	Concentration, g/L (meq/L)						
	Cl ⁻ (2)	Br ⁻ (3)	SO ₄ ⁻ (4)	Na ⁺ (5)	Ca ⁺⁺ (6)	Mg ⁺⁺ (7)	K ⁺ (8)
1	0.38 (10.72)	—	0.42 (8.75)	0.44 (19.13)	<0.01 (<0.50)	<0.01 (<0.82)	<0.01 (<0.25)
2	0.23 (6.49)	—	0.34 (7.08)	0.32 (13.91)	<0.01 (<0.50)	<0.01 (<0.82)	<0.01 (<0.25)
3	0.30 (8.46)	—	0.43 (8.96)	0.40 (17.39)	<0.01 (<0.50)	<0.01 (<0.82)	<0.01 (<0.25)
4	0.82 (23.13)	—	0.44 (9.17)	0.62 (26.96)	0.02 (1.00)	<0.01 (<0.82)	<0.01 (<0.25)
5	0.80 (22.50)	1.33 ^a (16.68)	0.44 (9.17)	0.89 (38.70)	0.04 (2.07)	0.01 (1.15)	0.17 ^b (4.44)

^aInitial Br⁻ concentration (@ t = 0) = 1.50 g/L.

^bInitial K⁺ concentration (@ t = 0) = 0.73 g/L.

TABLE 6. Summary of Experimental Diffusion Coefficients for Cl⁻

Sample number (1)	Experimental diffusion coefficient @ 10° C (cm ² /s) (2)	Tortuosity factor (3)
1	1.5 × 10 ⁻⁰⁶	0.15
2	1.5 × 10 ⁻⁰⁶	0.15
3	2.0 × 10 ⁻⁰⁶	0.20
4	not determined	—
5	2.0 × 10 ⁻⁰⁶	0.20

plained in terms of uncertainty in Cl⁻ concentration. For this test, the measured concentrations for the upper one-half to two-thirds of the sample fall below the theoretical values. It is considered that this deviation from the theoretical diffusion profiles is primarily due to moisture uptake from the distilled water reservoir, which contributes to a decrease in the chloride concentration within the sample. For example, based on (7), an increase in moisture content from 9% (background) to about 11%, as noted for sample 4, would result in a 20% decrease in Cl⁻ pore water concentration. In so doing, the moisture content increase would have influenced the diffusion process itself, since diffusion is driven by the concentration gradient. Since this additional dilution of chloride pore water concentration is not accounted for by the theoretical model, there is poor agreement between the theoretical curves and the measured concentration data. Hence, a Cl⁻ diffusion coefficient is not reported for this sample.

As previously indicated, the measured Cl⁻ concentration profiles and the theoretical analysis are based on the assumption that the entire moisture content, and, hence, the total porosity, is available to the diffusing Cl⁻ ions [i.e., $n' = n$ in (4)]. To assess the validity of this assumption, consideration is given to the distribution of pore size within the rock in comparison to the hydrated diameter of a Cl⁻ ion. As determined by a Micromeritics Mercury Porosimeter, the distribution of pore sizes in the range 300–0.006 μm in diameter is shown for sample 2 in Fig. 4. The distribution shows a sharp

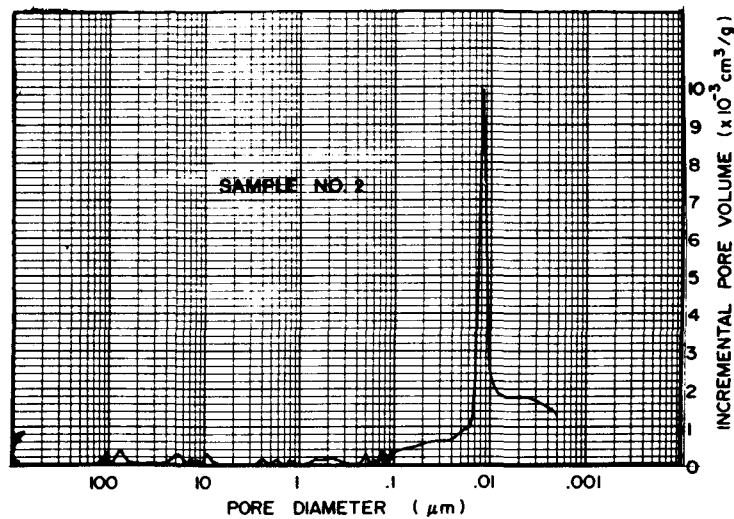


FIG. 4. Pore Size Distribution for Sample 2 (by Mercury Porosimeter)

TABLE 7. Pore Size Distribution for Bison Mudstone*

Pore diameter (μm) (1)	Total porosity (%) (2)	Method of analysis (3)
300-0.06	~10%	Micromeritics Mercury Porosimeter
0.06-0.006	~66%	Micromeritics Mercury Porosimeter
0.006-0.002	~14%	Quantachrome Automated Gas Adsorption System
	$\Sigma = 90\%$	

*Obtained on freeze-dried mudstone.

pore size mode centered at about $0.03 \mu\text{m}$. Based on this data as well as pore size data obtained from a Quantachrome Automated Gas Adsorption System (capable of measuring pore sizes in the range $0.06-0.002 \mu\text{m}$), the percentage of total porosity corresponding to various ranges in pore diameter is indicated in Table 7. The data shows that the total porosity is largely derived from pores $0.06-0.002 \mu\text{m}$ in diameter, and that approximately 10% of the total porosity is derived from pores outside the range of measurement (i.e., $>300 \mu\text{m}$ and/or $<0.002 \mu\text{m}$). Considering that the hydrated diameter of chloride is only about $0.0007 \mu\text{m}$ (Horvath 1985), it would seem reasonable to assume that essentially all of the pore spaces are large enough to accommodate the fully hydrated diameter of chloride. Since the rock contains some smectite (e.g., see Table 2), consideration is also given to the possibility that some pores may consist mostly of clay double-layer water from which chloride would be expelled. Based on the theory outlined by Mitchell (1976), the double-layer thickness for a sodium-saturated smectite in a solution having a total ion concentration of 0.3 Molar

s about 0.0007 μm . For a calcium-saturated smectite, the double-layer thickness would be about 0.0003 μm . Since these thicknesses are small relative to the range in pore size, it seems that essentially all of the pore-water, and, thus, the total porosity, is available to the diffusing Cl^- ions.

Determination of Bromide Diffusion Coefficient

Fig. 5 shows the bromide concentration profile obtained for sample 5, which was tested using a reservoir solution of 2.2 g/L KBr in distilled water. The initial Br^- concentration obtained on background slices cut above and below the sample was below the detection limit of the wash technique (i.e., <0.03 g/L). Therefore, the initial background concentration profile for Br^- was considered to be zero. As a check on the experimental methods, the percentage recovery for Br^- at the end of the test was calculated as 95%. As for chloride, calculation of the bromide concentration data involved the assumption that essentially all of the moisture content is available to the Br^- ions. Since Br^- has a hydrated diameter similar to that of Cl^- , the previous discussion suggesting the validity of this assumption for Cl^- would also apply for Br^- .

The Br^- concentration profile given in Fig. 5 shows that Br^- migration has extended to the bottom of the sample. In order to maintain charge balance, the diffusion of Br^- into the rock is coupled with the inward diffusion of K^+ , despite the fact that the initial K^+ concentration in the source reservoir (0.73 g/L) is less than the initial K^+ pore water concentration (2.10 g/L, Table 3). This is indicated by the decrease in K^+ concentration in the reservoir, from an initial value of 0.73 g/L to a value of 0.17 g/L at the end of the test (see Table 5).

Comparison of the theoretical curves and experimental data in Fig. 5 indicates that the measured Br^- pore water concentration for the top three slices falls below the theoretical curves by an amount that cannot be explained by the uncertainty in Br^- pore water concentration. It is believed that the deviation between experimental and theoretical profiles is primarily due to interactions between Br^- and cations naturally occurring in the sample pore water. In explanation, as K^+ migrates into the sample with Br^- , it adsorbs onto the clay exchange sites at the expense of Na^+ (see Fig. 6). The desorbed Na^+ must then help provide charge balance for Br^-

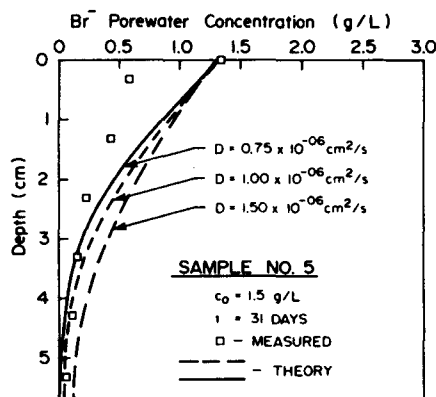


FIG. 5. Bromide Pore Water Concentration Variation with Depth for Sample 5

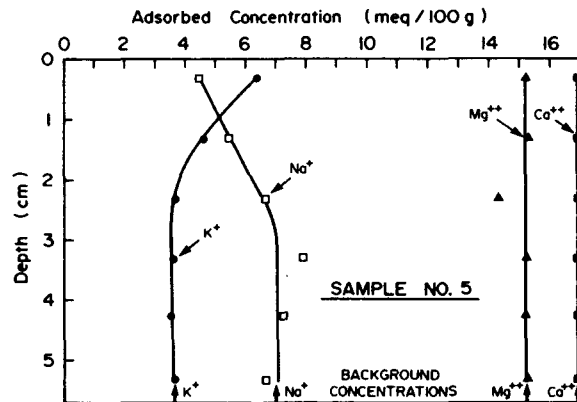


FIG. 6. Adsorbed Concentration Variation with Depth for Sample 5 ($t = 31$ Days)

diffusing towards the base of the sample. However, because Na^+ experiences an upward concentration gradient (much stronger in magnitude than that for Br^-), some of the Br^- that is coupled with Na^+ would be driven back up into the reservoir. This would reduce the net Br^- flux into the sample, and, in turn, would reduce the Br^- pore water concentration relative to that predicted by the theoretical model. For this reason, a diffusion coefficient for Br^- is not given.

SUMMARY AND CONCLUSION

This paper has presented an estimation of the chloride diffusion coefficient and the tortuosity factor on samples of intact Bison mudstone using a simple nonsteady-state diffusion test technique. For the conditions examined, it is concluded that the diffusion coefficient for chloride at a temperature of 10°C ranged from 1.5 to $2.0 \times 10^{-6} \text{ cm}^2/\text{s}$, which corresponds to a tortuosity, τ , ranging from 0.15 to 0.20 . The tortuosity factor obtained from the tests may be useful in estimating the diffusion coefficient of other species in similar rock, provided that the species' diffusion coefficient in aqueous solution is known.

Based on pore size measurements, thickness of clay double layers, and the hydrated ionic diameter for chloride, the effective porosity of the Bison mudstone with respect to the diffusion of chloride is considered to be approximately equal to the total porosity determined from the moisture content.

Comparison of the moisture content profiles before and after the diffusion test indicated that some moisture uptake had occurred in all samples. For four out of the five samples tested, the measured increase in moisture content corresponded to a percentage volume change ranging from 0.23% to 0.56% . Since the Cl^- concentration profiles for these samples was adequately fitted by the Fickian diffusion theory, it is suggested that the volume change did not significantly affect the developed diffusion profile at the end of the test. For one sample, however, the percentage volume change (1.64%) was significantly larger than the others. The additional influx of water for this sample decreased the Cl^- pore water concentration by an amount that was significant relative to the dilution generated by Cl^- diffusion up into

the reservoir. This resulted in a lack of agreement between the observed Cl^- concentration profile and the theoretical profiles. A diffusion coefficient for this specimen was not given.

Finally, for a single test, the distilled water reservoir was spiked with 2.2 g/L of KBr in an attempt to determine the diffusion coefficient and corresponding tortuosity factor for Br^- diffusing into the sample, simultaneously with Cl^- diffusing out. For this case, the Br^- concentration profile at the end of the test could not be fitted by the theoretical model due to interactions between Br^- and other naturally occurring cations diffusing out of the sample.

ACKNOWLEDGMENTS

The work reported in this paper forms part of a general program of research into the migration of contaminants through barriers being conducted in the Geotechnical Research Center of the University of Western Ontario. The writers are indebted to Ontario Hydro Research Division (Rock Science Section) for conducting part of the pore size analysis. The writers would also like to express their appreciation to John A. Cherry and Stan Feenstra for initiating this study.

APPENDIX I. REFERENCES

- American Institute of Physics Handbook*. (1972). 3rd Ed., McGraw-Hill, New York, N.Y.
- Barone, F. S., Rowe, R. K., and Quigley, R. M. (1990). "Laboratory determination of chloride diffusion coefficient in an intact shale." *Can. Geotech. J.*, 27(2), 177-184.
- Chhabra, R. (1975). "The measurement of the cation exchange capacity and exchangeable cations in soils: A new method." *Proc. of the Int. Clay Conf.*, 439-449.
- Freeze, R. A., and Cherry, J. A. (1979). *Groundwater*. Prentice Hall, Englewood Cliffs, N.J.
- Horvath, A. L. (1985). *Handbook of aqueous electrolyte solutions*. John Wiley and Sons, New York, N.Y.
- Mitchell, J. K. (1976). *Fundamentals of Soil Behaviour*. John Wiley and Sons, New York, N.Y.
- Quigley, R. M., Yanful, E., and Fernandez, F. (1987). "Ion transfer by diffusion through clayey barriers." *Proc. of ASCE Specialty Conf. on Geotechnical Aspects of Waste Disposal*, ASCE, New York, N.Y.
- Rowe, R. K., and Booker, J. R. (1985). "1-D pollutant migration in soils of finite depth." *J. Geotech. Engrg.*, ASCE, 111(4), 479-499.
- Rowe, R. K., and Booker, J. R. (1989). "A semi-analytic model for contaminant migration in a regular two or three dimensional fracture network: Conservative contaminants." *Int. J. Numer. Anal. Methods Geomech.*, 13, 531-550.
- Rowe, R. K., and Booker, J. R. (1990). *POLLUTE - 1D pollutant migration through a non-homogeneous soil: Users manual*. Geotech. Res. Ctr., Univ. of Western Ontario, London, Ontario, Canada.
- Wilke, C. R., and Chang, P. (1955). "Correlation of diffusion coefficients in dilute solutions." *AIChE J.*, 1(2), 264-270.

APPENDIX II. NOTATION

The following symbols are used in this paper:

c = species concentration in pore water;

c_o = species concentration in reservoir at start of test;
 c_s = species concentration in wash supernatant;
 c_T = species concentration in reservoir;
 D = species diffusion coefficient in porous media;
 D_o = species diffusion coefficient in pure aqueous solution;
 f_T, f_B = mass flux of dissolved species across top and bottom of sample, respectively;
 H_f = equivalent height of distilled water above sample;
 m = mass of oven-dried sample used for measuring Cl^- pore water concentration;
 n = total porosity of porous media;
 n' = porosity available for dissolved species diffusion (effective porosity);
 t = time;
 V = volume of wash supernatant;
 w = moisture content;
 z = depth;
 ρ = density of pure water at 22° C; and
 τ = tortuosity of porous media.